Original Paper

Radiation-induced defects in CoO- and NiO-doped fluoride, phosphate, silicate and borosilicate glasses

Doris Möncke and Doris Ehrt

Otto-Schott-Institut für Glaschemie, Friedrich-Schiller-Universität Jena, Jena (Germany)

The influence of cobalt and nickel on the formation of irradiation-induced defects was studied in fluoride, phosphate, silicate and borosilicate glasses. Sample plates of high-purity glasses, undoped and doped with 0.3 mol% CoO and NiO, respectively, were irradiated with UV lamps and with X-rays. The subsequent defect centers, formed at ppm levels, were characterized by EPR and optical UV-VIS spectroscopy.

X-ray irradiation caused stronger solarization (excitation of inner electrons) than UV lamp irradiation (selective excitation of valence electrons). More defects were formed in doped than in undoped glasses, generally stronger for Co^{2+}- than for Ni^{2+}-doped glasses and especially strong in glasses of high optical basicity where Co^{2+} and Ni^{2+} were tetrahedrally coordinated. Co^{2+} was photooxidized to $(Co^{2+})^{+}$ in all glasses, replacing some of the intrinsic hole centers (HC), with $(Co^{2+})^{+}$ in tetrahedral coordination: charge transfer band <400 nm, and $(Co^{2+})^{+}$ in octahedral coordination: two bands between 300 and 450 nm. Ni^{2+} was photooxidized in the (boro-)silicate glasses, which all had a higher basicity, but was photoreduced in the fluoride-phosphate glasses of low basicity. Photoreduced $(Ni^{2+})^{-}$ was found in the phosphate glass of medium basicity only after X-ray irradiation. The photoionized nickel species also displayed distinct EPR signals, with $(Ni^{2+})^{+}$: several bands from 700 to 200 nm, g=2.10; and $(Ni^{2+})^{-}$: 330 nm, g_1=2.08 and g_2=2.26.

1. Introduction

Radiation-induced defects in glasses require high attention due to the intensified applications of stronger lamps and lasers, working at increasingly shorter wavelengths. Solarization describes the effect of decreased transmission in the UV and VIS range due to color centers generated by irradiation. These color centers, or defects, evolve in ppm concentrations when the irradiation is sufficient to ionize the glass. The defects can be divided into negatively charged electron centers (EC) and corresponding positively charged hole centers (HC) [1].

Cobalt- and nickel-doped glasses are used as optical filters. They show high transmission from 250 to 400 nm and a strong absorption between 450 and 700 nm. Cobalt and nickel are polyvalent as well as polycoordinated ions. These ions are rarely seen in glasses in any other oxidation state than +2. In this state, the coordination is either tetrahedral (T_d) or octahedral (O_h) depending strongly upon the glass matrix. The differently coordinated ions show distinctive spectra and therefore different colors, leading to their use as structure indicators [2].

Received 31 October 2001.

Presented in German at: 75th Annual Meeting of the German Society of Glass Technology (DGG) in Wernigerode (Germany) on 22 May 2001.

The optical basicity (Λ) of the glass is a measure of the electron donor power of the glass matrix [3 to 5]. It is proportional to the electron density on the oxide (-2) and can be correlated to the coordination of the Co^{2+} and Ni^{2+} ions [6]. In more acidic glasses, the ions show ionic-bonded octahedral coordination while covalent-bonded tetrahedral coordination prevails in high-basicity glasses.

The kinetics of formation and recovery of induced defects in fluoride-phosphate (FP) and phosphate glasses irradiated with lamps and lasers have been intensively studied [7 to 9]. The numerous induced intrinsic defects were characterized by EPR (electron paramagnetic resonance) and optical spectroscopy. Studies on the intrinsic defects in silicate glasses concentrated on pure quartz glass and included only few borates. Some review articles that can be found are stated in [10 and 11].

Solarization by different radiation sources has already been studied in several CoO- and NiO-doped model glasses discussed separately in previous papers [12 to 15]. The model glasses studied range from the acidic fluoride-phosphates FP4 and FP20, over the strontium metaphosphate P100 and the borosilicate NBS2 of medium basicity, to the high-basicity borosilicate and silicate glasses NBS1 and NCS (table 1). Based on the former investigations on intrinsic defect formation and the

Table 1. Composition (in mol%) and characteristics of the model glasses studied

	NCS	NBS1	NBS2	P100	FP20	FP4
	74 SiO_2 10 CaO 16 Na_2O	74 SiO_2 10 B_2O_3 16 Na_2O	74 SiO_2 21 B_2O_3 4 Na_2O 1 Al_2O_3	100 $Sr(PO_3)_2$	20 $Sr(PO_3)_2$ 80 { AlF_3, MgF_2, SrF_2, CaF_2	4 $Sr(PO_3)_2$ 96 { AlF_3, MgF_2, SrF_2, CaF_2
Λ_{th} [1]	0.57	0.53	0.48	0.46	0.38	0.35
Λ_{Pb} [2]				0.47	0.45	0.34
ΣFe in ppm	5	5	5	8	10	10
Fe^{3+} in ppm				5	6	6
T_g in °C	530	550	440	510	490	440
n_e	1.52	1.51	1.47	1.56	1.50	1.43
ϱ in g/cm³	2.49	2.45	2.18	3.15	3.51	3.46
coordination	T_d	T_d	O_h	O_h	O_h	O_h
color [3] Co	blue	blue	violet	violet	violet	violet
color [3] Ni	brown	violet	violet	yellow-green	amber	amber
solarization	very strong	very strong	less pronounced	less pronounced	less pronounced	less pronounced

[1] Theoretical optical basicity according to Duffy [3 and 4].
[2] Optical basicity values experimentally determined via the Pb^{2+} indicator ion as found by Seeber [5].
[3] NiO and CoO were doped in concentrations of 0.3 mol%, respectively.

already published results on solarization in CoO- and NiO-doped glasses, this paper will characterize the extrinsic defects found and will discuss their occurrence for the different model glasses.

2. Experimental procedures

The (boro-)silicate glasses were melted in batches of 250 g in platinum crucibles in an electric furnace at 1450 °C for 3 h and quenched in water before they were remelted at 1450 °C for another 2 h (1650 °C were used for NBS2). 100 g batches of the FP glasses were melted in platinum crucibles in an electric furnace at 1000 °C and 100 g batches of the phosphate glasses at 1350 °C using SiO_2 crucibles. The glasses were all cooled in graphite molds from 550 °C to room temperature with a cooling rate of about 30 K/h.

Alkaline-rich cesium-barium-silicate glasses (CBS50: 50 SiO_2, 40 Cs_2O, 10 mol% BaO) were also prepared for comparison of the optical spectra. These glasses of very high optical basicity contained Co^{3+} and Ni^{3+} and were melted in SiO_2 crucibles at 1300 °C for 1 h in batches of 30 g. As these glasses are highly hygroscopic, 1 to 3 mm thick polished sample plates were embedded between two polished quartz plates with the sides sealed with silicon to protect the glasses from the atmosphere.

All model glasses were melted as undoped base glasses, and doped with 0.3 mol% CoO and NiO, respectively, as well as with 0.15 mol% CoO and NiO simultaneously. The reagents SiO_2, $CaCO_3$, H_3BO_3, $Al(OH)_3$, Na_2CO_3, $Sr(PO_3)_2$, AlF_3, SrF_2, CaF_2, MgF_2, $Ba(NO_3)_2$ and Cs_2CO_3 of high purity were used for melting so that the iron content of the glasses could be kept as low as 5 to 10 ppm.

Polished plates with the dimensions (10 × 20 × 2) mm^2 were irradiated with lamps and 1 mm thick samples were also irradiated with X-rays (table 2). The 1 kW HgXe lamp works in a sun simulator from Oriel Instruments, Stratford, CT (USA) and continuously emits a wide spectrum from the UV to the NIR. The spectral power density of this lamp is about 1500 W/m^2 between 230 to 280 nm. The samples were placed at a 10 cm distance from the radiation source and irradiated for up to 100 h to ensure that defect formation reached the saturation level. The HOK lamp, applied at SCHOTT Glas, Mainz (Germany), is a high-pressure mercury lamp with a similar spectral power density. However, due to its greater emission spectrum, which covers also the range up to 180 nm, stronger defects can be expected, as most of the solarization damage is caused by the high-energy radiation of shorter wavelengths. For X-ray irradiation, the sample plates were subjected to a copper-cathode radiation of 10 kW (50 kV, 200 mA) at a distance of 80 cm. In this case irradiation lasted only 16 h.

UV-VIS-NIR spectra were used to characterize the glasses and to observe the irradiation-induced defects. A double-beam spectrophotometer (UV-3102 PC, Shimadzu, Tokyo (Japan)) was employed, recording the extinction $E = \lg(I_0/I)$ with an error <1 %. The internal extinction was later standardized to a nominal path length (d) of 1 cm. The induced extinction ($\Delta E/d$), or change of optical density caused by the irradiation, is used to describe the defects. EPR spectroscopy was used as a second, independent analytical method. For comparison the glasses were also analyzed with the addition of the spin standard dpph (1.1-diphenyl-2-piterylhydroxyl). All spectra displayed within one series were taken from samples of the same dimension and as such

Table 2. Irradiation sources

irradiation source	irradiation	spectral performance	irradiation time in h
XeHg lamp	continuous UV-NIR	I: 1500 W/m^2 for 230 to 280 nm	100
HOK lamp	continuous UV-NIR	I: 1500 W/m^2 for 190 to 280 nm	100
X-ray	Cu cathode	10 kW (50 kV, 200 mA)	16

Note: I = spectral power density.

could be standardized. The EPR spectrometer used (ESP 300 E, Bruker, Karlsruhe (Germany)) worked with a frequency band of $\nu \approx 9.78$ GHz. The resolved Gaussian bands of the induced optical spectra were correlated with defect centers detected by EPR and optical spectra of thermal recovery measurements. Band separation of the diverse spectra was accomplished on the computer with customary auxiliary software.

Information for band separation and the assignment of the bands and EPR signals was based on literature data and additional experiments. Many intrinsic defects have already been characterized in some detail, especially in FP and phosphate glasses [7 to 9]. Bands and EPR signals of different cobalt or nickel species can be found in the literature [16–28]. Thermal recovery experiments were routinely performed on irradiated samples. Soft heating of the samples gave more information for the task of band separation and classification of the defect centers. Besides the photooxidized iron, normally all irradiation-induced defects recover wholly before the temperature reaches T_g. Some bands, like those stated for $(Ni^{2+})^+$, were set to account for the smallest set of bands (of similar ratios, form and half-width amplitudes), which are needed for the band simulation of a wide range of similar but not altogether identical glasses after different irradiation or thermal recovery treatments. These bands were further compared to literature data, EPR results and their correlation with the intrinsic defects.

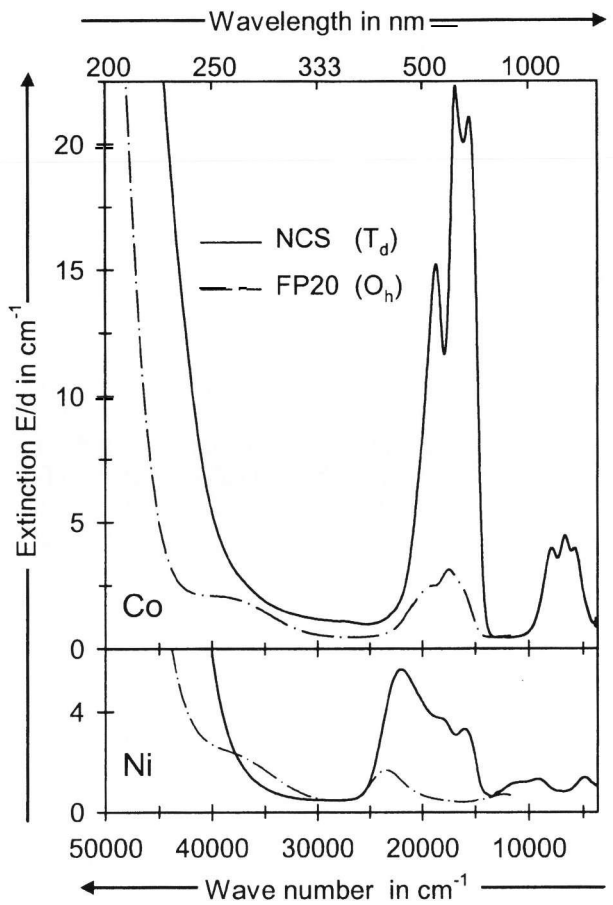

Figure 1. Optical spectra of two glasses doped with 0.3 mol% CoO and NiO, respectively; Co^{2+} (top) and Ni^{2+} (bottom) are primarily tetrahedrally coordinated in NCS glass (—) and octahedrally coordinated in FP20 glass (–·–).

3. Results and discussion

The glass NCS is a common soda-lime-silicate glass. Exchange of CaO for B_2O_3 yields the borosilicate glass NBS1. Replacing further Na_2O by B_2O_3 until the ratio of the boric oxide anomaly is reached gives the second borosilicate glass NBS2, which differs significantly from the NBS1 glass by its lack of nonbridging oxygens and a higher ratio of BO_3 units over BO_4 tetrahedra. The small amount of Al_2O_3 prevents the immiscibility of the ternary composition of the glass NBS2, which can be seen as a model for the glasses Duran®, or Borofloat® as can NBS1 for the optical glass BK7. NBS1 and NCS are further distinguished from the medium basicity NBS2 by their higher optical basicity, causing Co^{2+} and Ni^{2+} in these glasses to be primarily tetrahedrally coordinated. The other three model glasses include a pure strontium metaphosphate glass P100 also of medium basicity and two fluoride-phosphate glasses of low optical basicity.

Figure 1 shows the optical spectra of the differently coordinated ions. Due to the different symmetries and thus d → d transition probabilities, the intensities of the bands of the tetrahedrally coordinated ions are up to 100 times higher than those of the octahedrally coordinated ions. As nickel strongly favours the octahedral over the tetrahedral coordination [16], even the high-basicity NCS glass displays a mixed spectrum of tetrahedral- and octahedral-coordinated Ni^{2+} ions. In FP20 glass cobalt and nickel show the typical spectra of an

octahedral coordination, as it is also found in the borosilicate glass NBS2 and the glasses FP4 and P100.

As many solarization-induced defect centers absorb strongly in the UV and VIS range, optical spectroscopy is a good tool for studying the formation of these defects. However, the bands of any evolving electron centers are usually found near the UV edge, where the dopants also absorb strongly, complicating the evaluation of the optical bands. Although Co^{2+}- and Ni^{2+}-compounds have been successfully investigated by EPR, Co^{2+} and Ni^{2+} in glass give no visible EPR signals and could only be detected at extremely low temperatures [17 and 18]. Since no signals seem to arise in glasses from Co^{2+} and Ni^{2+}, EPR spectroscopy permits the detection of paramagnetic EC and HC in glasses at room temperature without interferences from the two dopants. One explanation for the absence of a Co^{2+} and Ni^{2+} signal might arise from a tetragonal or trigonal distortion of their complexes, leading to low-lying excited states instead of the normally found degeneracy of octahedral complexes. The low-lying excited state results from minimal quenching of orbital motion and gives rise to exceedingly short relaxation times and large spectral anisotropies. The latter causes the particular smear-out of the spectra observed in glasses, while the short relaxation times lead to the enormous line widths at practical laboratory temperatures [19]. (Preirradiated CoO-doped model glasses were analyzed at temperatures between 4 and 77 K and a broad signal was found at g-values between 4 and 7.)

When comparing such different irradiation sources it might be important to stress that high-energy X-ray irradiation will excite all kinds of possible effects in the glasses, while lamp irradiation excites only a small number of well-defined defects. Therefore, extrapolation from X-ray to long-term UV lamp solarization is not advisable. The results of X-ray irradiation should be discussed nevertheless, as this method partly led to new defects and the intensities of the defects known from lamp irradiation were several magnitudes higher.

Solarization in the glasses doped simultaneously with CoO and NiO can be explained by the combination of the defects found in the monodoped glasses. Further discussion will therefore concentrate on the undoped- and monodoped-melted glasses. Because of the high analogies in defect formation for both glasses containing Co^{2+} and Ni^{2+} in tetrahedral coordination, the glasses NCS and NBS1 will be discussed only on the example of the glass NCS. As solarization in the phosphate and FP glasses can be explained in a similar way as well, these defects will only be briefly discussed on the example of the glass FP20. A more detailed analysis of the solarization defects in the CoO- and NiO-doped phosphate and FP glasses can be found in already published articles [12 and 13].

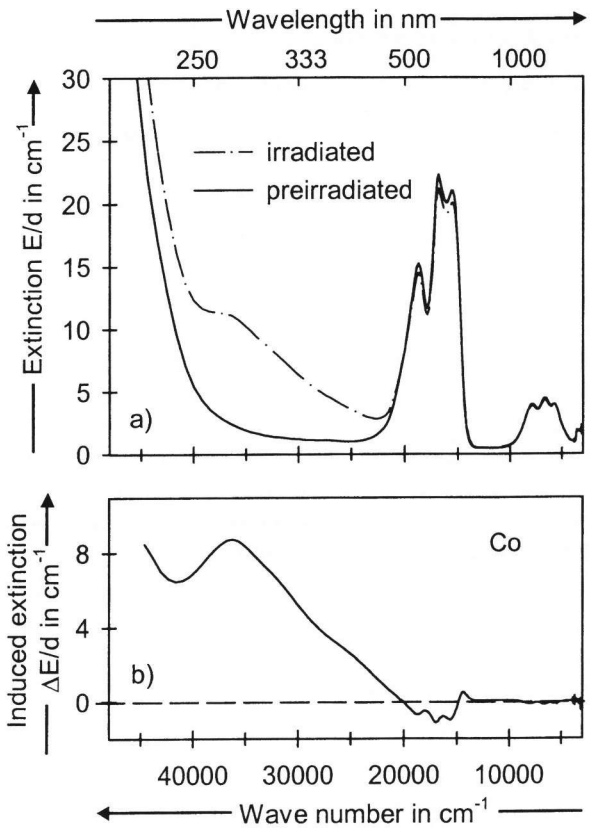

Figures 2a and b. CoO-doped NCS glass; a) optical spectra before (—) and after (–·–) 100 h irradiation with the XeHg lamp, b) difference spectrum of the irradiated and preirradiated glass renders the induced optical spectrum of the defects.

3.1 The (boro-)silicate glasses NCS and NBS1

These two glasses showed after irradiation with the weak HgXe lamp by far the strongest induced extinctions of all the doped glasses. Figures 2a and b and 3a and b show the spectra of the doped glasses before and after 100 h irradiation as well as the difference spectra displaying the spectra of the irradiation-induced defects.

In the CoO-doped glass a strong induced absorption can be seen below 400 nm. Further a small negative absorption at the position of the tetrahedral Co^{2+} bands is observed. For the NiO-doped glass the strong induced absorption is limited to shorter wavelengths. However, as for CoO-doped glasses, changes in the induced absorption are found at longer wavelengths as well. Detailed studies of these changes imply a simple transformation from one Co^{2+} species into a defect center, and a more complex transformation for nickel, where more than one Ni^{2+} species might be involved. For example two differently coordinated Ni^{2+} species would contribute with different kinetics in the defect formation process [12].

Figure 4 shows the EPR spectra of the doped and undoped NCS glasses after XeHg lamp and after X-ray irradiation. All EPR spectra of the irradiated glasses studied are dominated by the signals of intrinsic HC. In

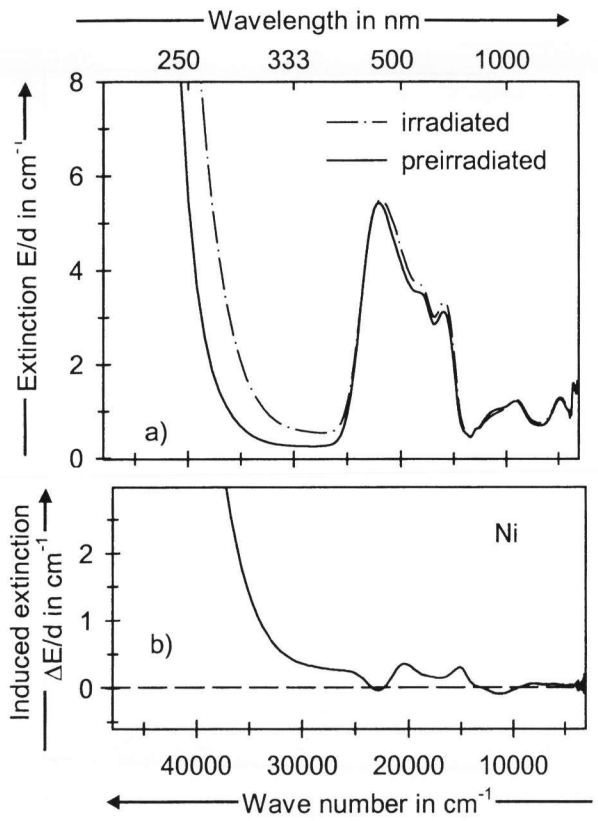

Figures 3a and b. NiO-doped NCS glass; a) optical spectra before (═) and after (−·−) 100 h irradiation with the XeHg lamp, b) difference spectrum of the irradiated and preirradiated glass renders the induced optical spectrum of the defects.

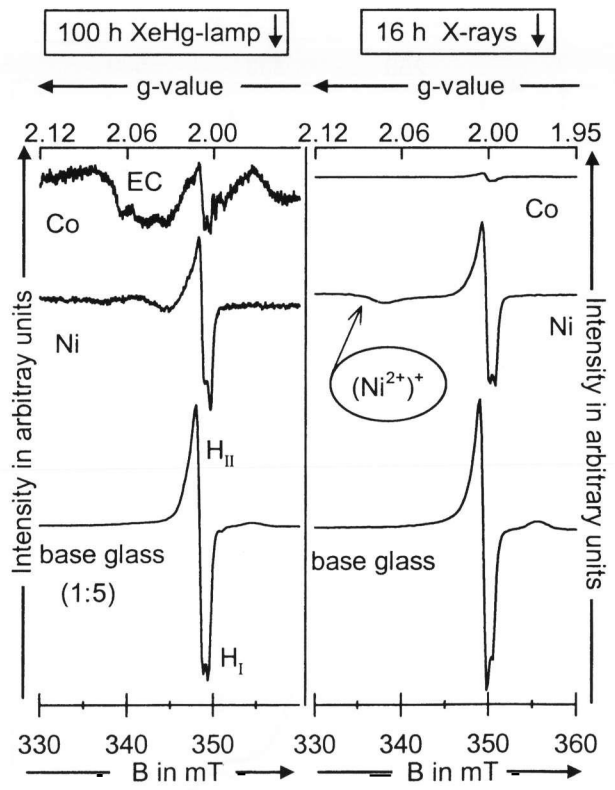

Figure 4. EPR spectra of undoped and doped NCS glasses after 100 h XeHg lamp irradiation (left) and 16 h X-ray irradiation (right); dpph-standardized, B=magnetic induction.

the silicate glasses the main signal actually consists of two overlapping signals with g-values around 2.0 from two different HC (H_I and H_{II}). These signals are significantly reduced in the doped glasses. After lamp irradiation only fragments of these HC signals are left in the CoO-doped glass, where only now the otherwise hidden weak EC signals become apparent. X-ray irradiation causes much stronger defect formation, which is also apparent in the much better signal-noise ratio in the second set of spectra. Even though the signal of the intrinsic HC is still very strong in the doped glasses, the intensity is much smaller than in the undoped glass. In addition a new signal at $g = 2.08$ appears in the NiO-doped glasses, a signal which can be related to an $(Ni^{2+})^+$ species [20 and 21]. Contrary to Co^{2+} and Ni^{2+}, Ni^{3+} as well as Ni^+ exhibit their own signals in glasses even at room temperature.

If the dopants replace the intrinsic HC by the formation of extrinsic defects, Co^{2+} and Ni^{2+} are photooxidized to $(Co^{2+})^+$ and $(Ni^{2+})^+$. To verify this process, the induced optical spectra of these glasses had to be compared to spectra of glasses containing Co^{3+} and Ni^{3+} in tetrahedral coordination. In figure 5a the optical spectrum of a cesium-barium-silicate glass CBS50 is shown. Because of the high alkali content and the high optical basicity of the big cesium ions, almost all the cobalt is present as Co^{3+} and only small amounts of Co^{2+} can be found. Co^{3+} has been prepared in like manner before by Dietzel and Coenen in extremely alkaline-rich alkali silicates [22]. Lamp irradiation of this glass does not easily cause further photooxidation. As most of the cobalt is already oxidized no strong additional photooxidation can be expected in this glass. The spectrum of the CBS glass containing Co^{3+} is in good agreement with the induced spectrum after X-ray (figure 5b) and lamp irradiation (figure 5c). The induced spectra differ primarily in their intensities and hardly in the form of the spectra, as long as the negative extinction of the tetrahedral Co^{2+} bands is taken into account.

Comparison of the NiO-doped CBS glass with the induced optical spectra is less forward (figures 6a to d). Even in the CBS glass with its high optical basicity a significant amount of Ni^{2+} (filled bands) is present together with Ni^{3+}, and at least the octahedral as well as the tetrahedral coordination have to be considered for both Ni^{3+} and Ni^{2+} (figure 6a). Contrary to the CoO-doped CBS glasses lamp irradiation of the NiO-doped glasses causes strong defect formation. The induced optical spectrum is shown in figure 6b. This spectrum shows a certain likeness to the spectrum in figure 6c, the induced spectrum of NiO-doped NCS glass after X-ray irradiation. If a decrease of Ni^{2+} bands is considered in the induced spectra after lamp irradiation (figure 6d), all spectra of figure 6a to d can be simulated with similar

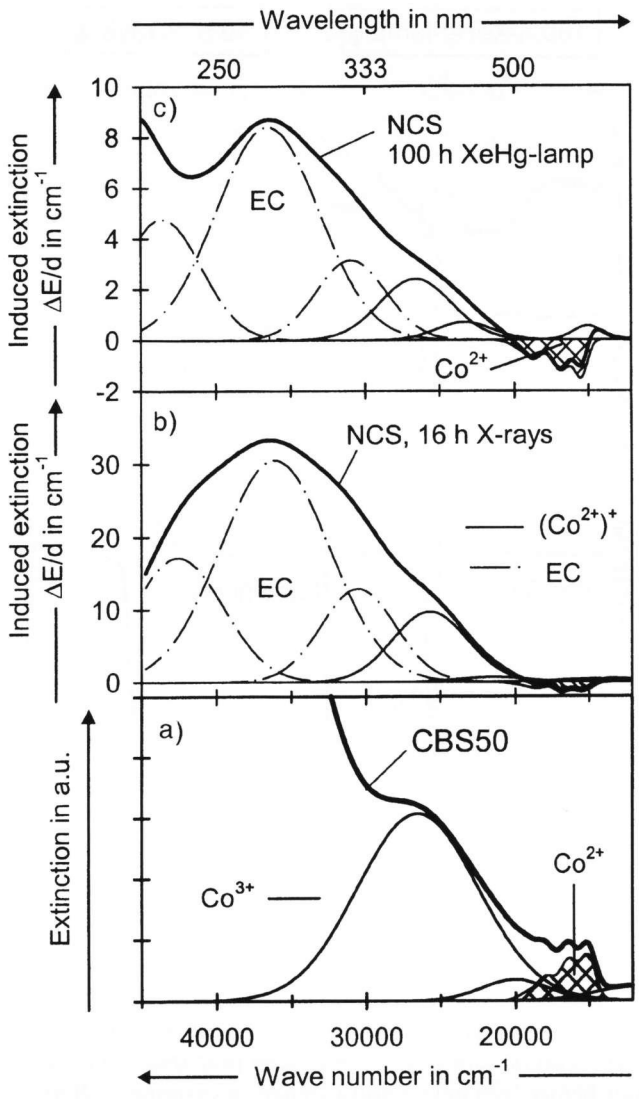

Figures 5a to c. Optical spectrum of CoO-doped CBS50 glass with Co^{2+} (xxxx) and Co^{3+} (═) a) in comparison to the induced optical spectra of CoO-doped NCS glass after b) 16 h of X-ray irradiation and c) 100 h of XeHg lamp irradiation.

sets of bands. References in the literature also show for the optical spectra of Ni^{3+} several badly resolved bands with decreasing intensities between 200 and 700 nm, and are thus in agreement with the assignments stated here [23 to 25].

The spectra of the doped NBS1 glasses are very similar to the spectra of the NCS glasses shown and can be explained accordingly. The same four main features can be found for all NBS1 and NCS glasses. First, a decrease of the tetrahedral Co^{2+} bands – and also less obviously in the Ni^{2+} bands – is seen with increasing irradiation. Second, the doped glasses display a much lower signal of intrinsic HC signals in their EPR spectra than the undoped glasses, even though the induced extinction was much higher in the doped than in the undoped glasses. Third, an EPR signal of Ni^{3+} is found after X-ray irradiation in all of the NiO-doped glasses. Fourth, there is a good agreement of the optical spectra of CBS glasses containing Co^{3+} with the induced optical spectra of the CoO-doped glasses. This agreement is also evident for

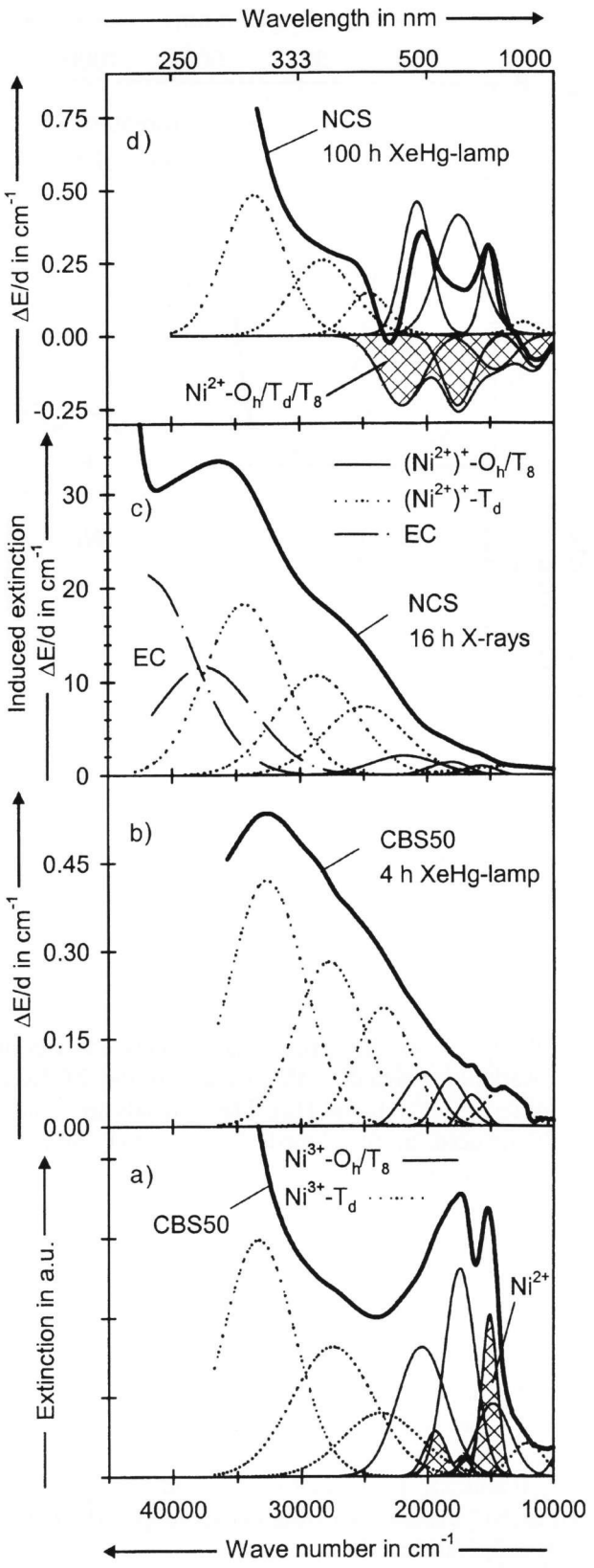

Figures 6a to d. Optical spectrum of NiO-doped CBS50 glass (figure a) in comparison to the induced optical spectra of the NiO-doped glasses b) to d) after 4 h XeHg lamp (CBS50), 16 h X-ray (NCS) and 100 h XeHg lamp irradiation (NCS).

the NiO-doped glasses, also less apparent due to the two simultaneously present coordinations. Together, these features show that in these glasses both dopants are

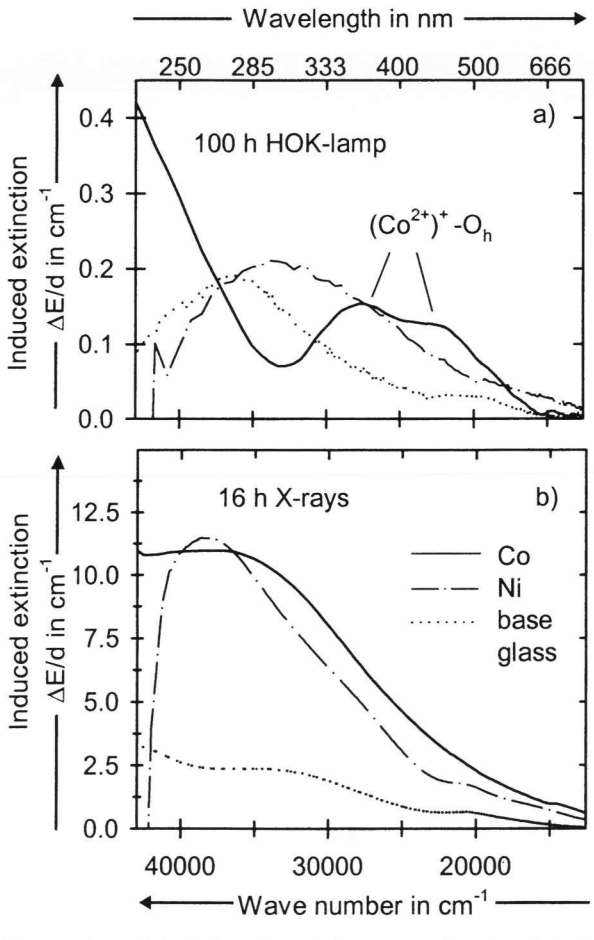

Figures 7a and b. Induced optical spectra of undoped (····), NiO-doped (−·−) and CoO-doped (═) NBS2 glass after a) 100 h HOK lamp and b) 16 h X-ray irradiation.

photooxidized and as extrinsic HC replace some of the intrinsic HC.

$$Co^{2+} + h\nu \rightarrow (Co^{2+})^+ + e^-$$

$$Ni^{2+} + h\nu \rightarrow (Ni^{2+})^+ + e^-$$

3.2 The low alkaline borosilicate glass NBS2

The glass NBS2, in which Co^{2+} and Ni^{2+} are octahedrally coordinated, showed overall a much lower degree of defect formation than the glasses NBS1 and NCS discussed before. Hardly any defects were found after irradiation with the weak XeHg lamp. However, irradiation by the stronger HOK lamp causes significant defects. Considering the thorough discussion of the extrinsic defects formed in the glass NCS, the similar characterization in the glass NBS2 can be summarized briefly given the apparent features in figures 7a and b and 8. Figure 7a shows the induced optical spectra after HOK lamp irradiation. The magnitude is very similar for all doped and undoped glasses, while in the analogous figure 7b, showing the induced spectra after X-ray irradiation, the doped glasses show a much stronger defect formation than the undoped glass. The EPR spectra in figure 8 are dominated again by the signal of the intrinsic HC. The characteristic quintet of the boron-related oxygen HC (BOHC) is easily recognizable. Contrary to the optical spectra, this signal significantly decreases in the doped glasses compared to the undoped base glass. As before the spectra of the NiO-doped glass displays the $(Ni^{2+})^+$ signal at $g = 2.08$. In analogy to the glasses NCS and NBS1 these spectra can also be interpreted by the photooxidation of Ni^{2+} and Co^{2+}. Furthermore, the characteristic form of the spectra of the CoO-doped glass in figure 7a, with two maxima between 300 and 500 nm, is characteristic of Co^{3+} in octahedral coordination [26 and 27].

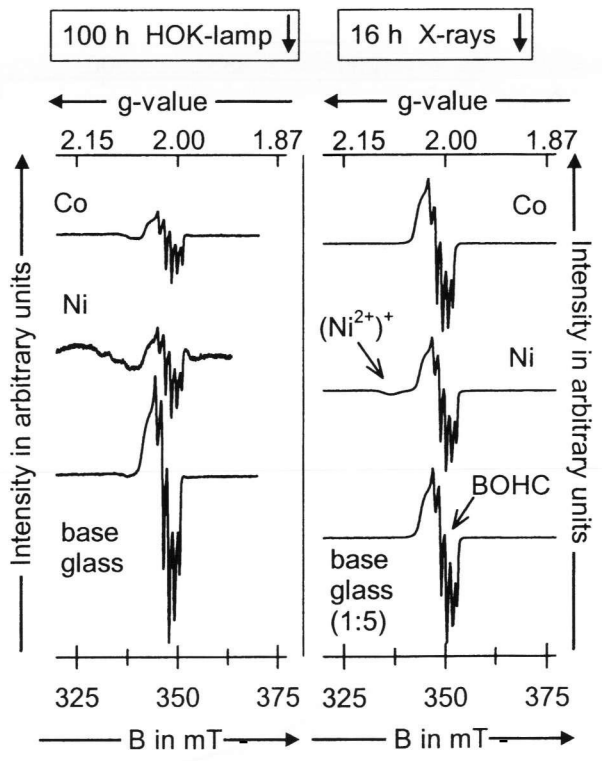

Figure 8. EPR spectra of CoO- and NiO-doped and undoped NBS2 glass after 100 h HOK lamp irradiation (left) and 16 h X-ray irradiation (right); dpph-standardized, B=magnetic induction.

The lower extent of defect formation in NBS2 compared to NBS1 and NCS can be explained by several means. The glass NBS2 shows a lower extent of intrinsic defect formation than the other two glasses. The lower optical basicity of NBS2 compared to NCS and NBS1 has a lower stabilizing effect on the photooxidized cobalt and nickel species and as both ions are octahedrally coordinated in the glass NBS2, the photooxidized species do not display the strong charge transfer (CT) transitions of the two tetrahedrally coordinated species.

3.3 The fluoride phosphate and phosphate glasses FP20, FP4 and P100

Because of the many similarities in their defect formation the metaphosphate and the FP glasses will be dis-

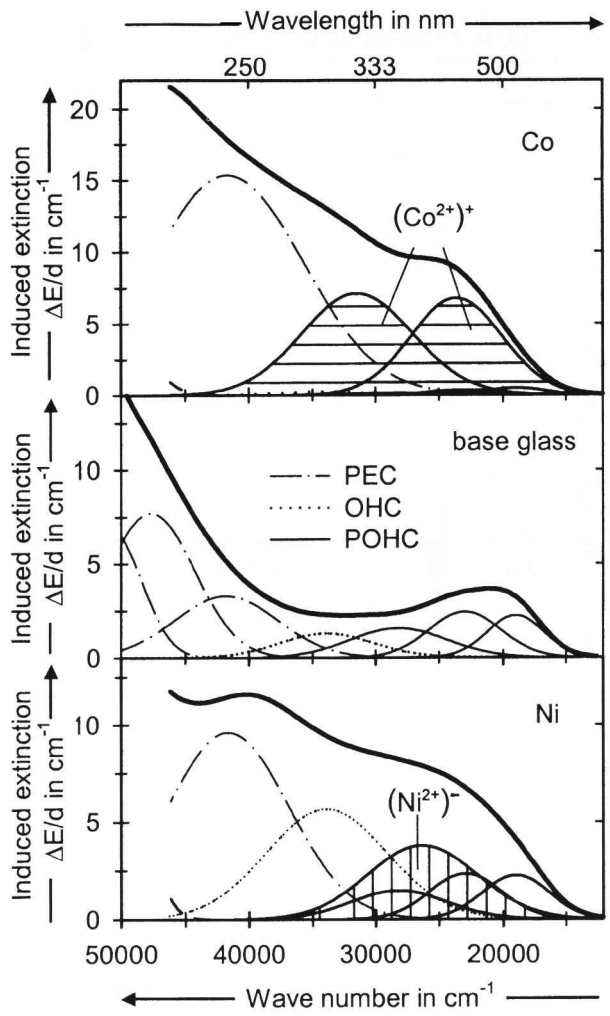

Figure 9. Induced optical spectra including band separation of CoO- and NiO-doped and undoped FP20 glass after 16 h X-ray irradiation.

cussed together, especially as solarization in these glasses has already been covered in more detail in [12 and 13]. P-bonded defects are more stable than are F-bonded ones. Therefore, FP glasses show the same P-related intrinsic defects than phosphate glasses. These defects have been intensively studied over the last years [7 to 9]. Phosphate glasses show distinct solarization even after irradiation with the weak XeHg lamp, but FP glasses are much more stable to solarization. Their stability increases with decreasing phosphate content. Thus after irradiation with the HOK lamp significant defects were found in the glass FP20 (20 mol% phosphates) but not in the glass FP4 (with only 4 mol% phosphates), the latter only showed apparent defects after X-ray irradiation.

Typical induced optical spectra of X-ray irradiated FP20 are displayed in figure 9. The base glass in the middle shows the bands of the intrinsic defects. The three bands of the phosphorous-bonded oxygen HC (POHC) are placed at longer wavelengths, and several bands connected with different EC are positioned near the UV edge. The induced optical spectra of the CoO-

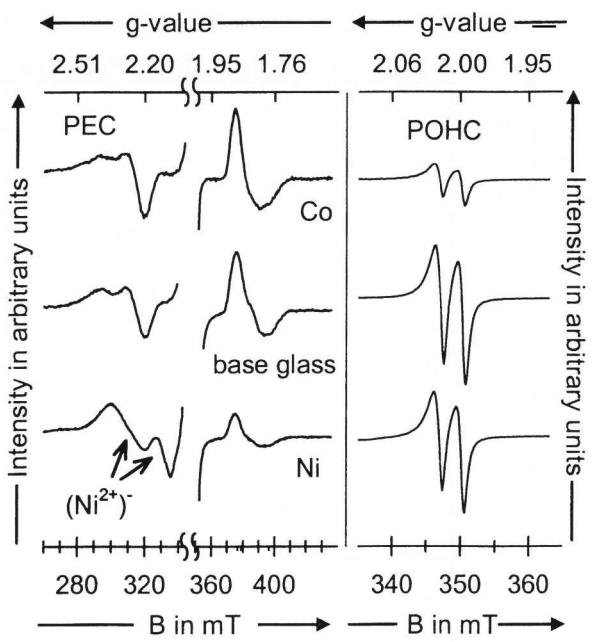

Figure 10. EPR spectra of doped and undoped FP20 glass after 16 h X-ray irradiation (dpph-standardized); magnified EPR spectra of the EC signals (left, POHC signals omitted) and segment of the EPR spectra showing the POHC signal (right).

doped glass clearly exhibits the two bands between 300 and 500 nm, which – as in the glass NBS2 – can be associated with photooxidized octahedrally coordinated $(Co^{2+})^+$. These extrinsic HC replace, as before in the other glasses, the intrinsic HC which is easily recognizable on the decreased POHC bands. The induced spectrum of the NiO-doped glass is more like the spectra of the undoped glass. Only one additional band at 350 nm can be seen, a band that according to the literature, can be related to $(Ni^{2+})^-$ [28]. Thus, Ni^{2+} is photoreduced forming an extrinsic EC, and the necessary charge balance is covered by the increase of the intrinsic oxygen related HC (OHC).

The EPR spectra validate the conclusions drawn from the optical spectra (figure 10). As in the other glasses the spectra are dominated by the signal of the intrinsic HC, in this case the sharp doublet of the POHC signal around $g = 2.0$. At higher and lower g-values other, much weaker signals are found that belong to the different intrinsic EC. All the EPR spectra show very similar features. The POHC signal is nevertheless significantly decreased in the CoO-doped glass compared to the undoped and NiO-doped glass, where the signal is essentially of the same intensity. Moreover, in the NiO-doped glass, additional signals are found at $g_1 = 2.26$ and $g_2 = 2.10$, which can be related like the band at 350 nm to a photoreduced $(Ni^{2+})^-$ [18, 29 to 31].

HOK lamp irradiation of the glass FP20 gives qualitatively the same bands and signals, only of much lower intensity, while in the FP4, as well as in both FP glasses irradiated with the weaker XeHg lamp, no significant defects can be found.

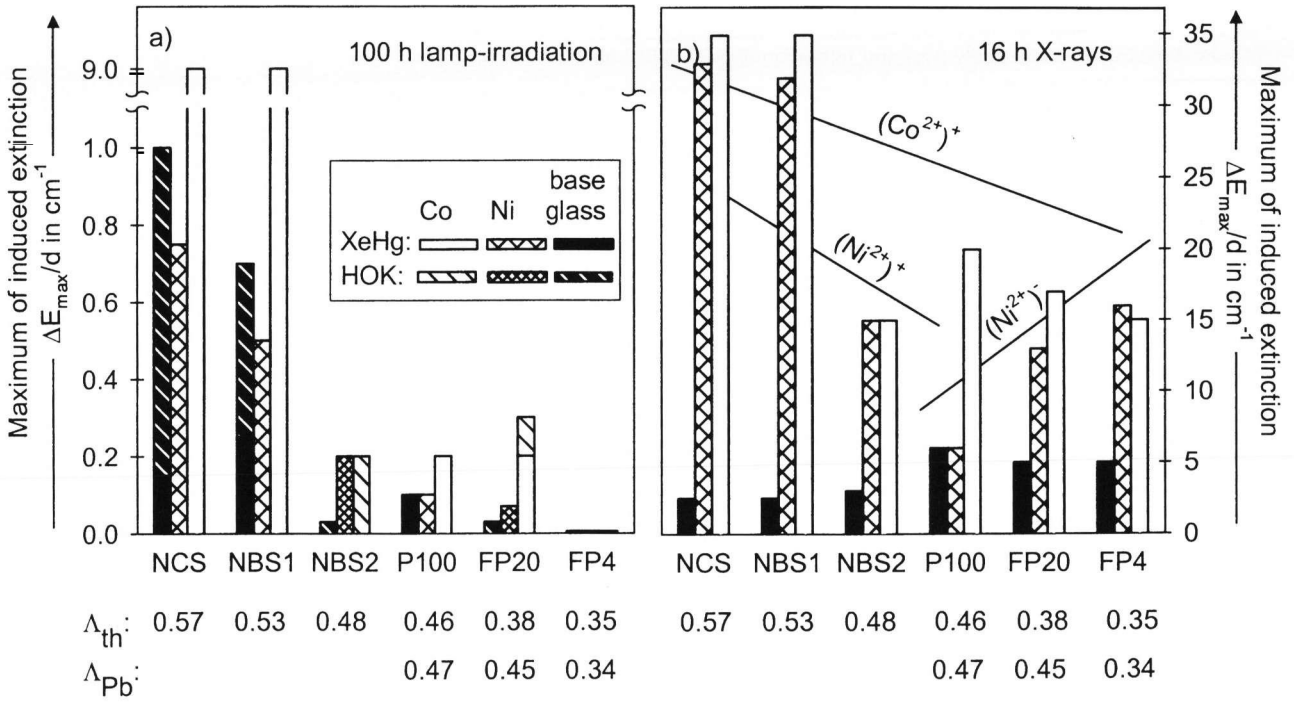

Figures 11a and b. Relative irradiation-induced extinction of the maximal absorption between 300 and 600 nm for the different model glasses after a) 100 h lamp irradiation (samples were either irradiated with the XeHg or the HOK lamp; if two glass samples were irradiated, the ΔE_{max} bar of the HOK lamp is placed behind that of the XeHg lamp); b) 16 h X-ray irradiation. (Λ_{th} optical basicity values calculated with the increment system according to Duffy [3 to 4], Λ_{Pb}: values derived experimentally with the Pb^{2+} indicator ion according to Seeber [5].)

X-ray irradiation of the metaphosphate glass P100 looks essentially similar to the spectra shown for FP20, however the photoreduction of Ni^{2+} to $(Ni^{2+})^-$ is markedly smaller in this glass, which has a higher optical basicity than the acidic fluoride phosphates. This is even more obvious in the glasses irradiated with the weak XeHg lamp. Contrary to the more stable FP glasses a considerable defect formation can be observed for all doped and undoped glasses. Principally the defects can be described in the same way as before. Co^{2+} is photooxidized, but no extrinsic defects are found in the NiO-doped glass, which only shows all the intrinsic bands and signals as found in the undoped base glass.

The EPR spectra of the irradiated P100 glass confirm the replacement of POHC by $(Co^{2+})^+$HC, while the intensity of the POHC signal stays the same for the undoped and the NiO-doped glass. After X-ray irradiation a weak signal of the $(Ni^{2+})^-$EC can be found in the NiO-doped glasses with a g-value of ≈ 2.1 [12 and 29].

4. Conclusions

This papers illustrates that irradiation-induced defects evolve in very different forms and intensities in a variety of CoO- and NiO-doped glasses. The strength of solarization depends on the radiation source, the coordination of the dopants as well as on the structure and optical basicity of the glass matrix.

While several optical bands and EPR signals could be associated with cobalt- and nickel-related extrinsic defects, others arose from intrinsic EC and HC. Many of these defects have been thoroughly analyzed in other studies [7 to 9], and the influence of cobalt and nickel on the form of the defects supports the previously reported interpretations for these intrinsic defects [7 to 9].

4.1 Irradiation source and solarization

X-ray irradiation not only excites the valence electrons as observed for lamp irradiation, but is also sufficient to ionize inner electrons. Thus defect generation was usually several magnitudes higher after X-ray than after lamp irradiation (figures 11a and b). In some glasses only X-ray irradiation led to significant defect formation (FP4) and in others, such as the NiO-doped P100 glass, X-ray irradiation caused defects that were not observed after lamp irradiation. Because of the larger emission spectrum, including high-energy wavelengths down to 190 nm, instead only to 230 nm as in the XeHg lamp, the HOK lamp causes stronger solarization than the XeHg lamp. Significant intrinsic defects are thus found for the glasses NBS2 or FP20, which are quite stable against XeHg lamp irradiation. While X-ray irradiation leads to more uniform strengths of the final solarization effects, a much higher degree of differentiation is found when the samples were irradiated with the more selective working lamps.

Table 3. Wave numbers of the irradiation induced bands and *g*-values for the different extrinsic defects found in the different model glasses doped with octahedrally (O_h) and tetrahedrally (T_d) coordinated cobalt and nickel ions

model glass	irradiation source	CoO-doped	λ in nm	NiO-doped	λ in nm	*g*-value
NCS and NBS1	XeHg lamp	T_d $(Co^{2+})^+$	385	T_d $(Ni^{2+})^+$	295, 370, 400 475[4], 590[4], 715[4]	2.08
	X-rays	T_d $(Co^{2+})^+$	385	T_d $(Ni^{2+})^+$	295, 370, 400	2.08
NBS2	XeHg lamp	$O_h(Co^{2+})^+$	–	O_h $(Ni^{2+})^+$	–	
	HOK lamp	O_h $(Co^{2+})^+$	–[5]	O_h $(Ni^{2+})^+$	250 to 400	2.08
	X-rays	O_h $(Co^{2+})^+$	370, 455	O_h $(Ni^{2+})^+$	250 to 400	2.08
P100	XeHg lamp	O_h $(Co^{2+})^+$	–	O_h $(Ni^{2+})^+$	–	
	X-rays	O_h $(Co^{2+})^+$	305, 400	O_h $(Ni^{2+})^-$	330	2.08
FP20	XeHg lamp	O_h $(Co^{2+})^+$	305, 400	O_h $(Ni^{2+})^+$	–	
	HOK lamp	O_h $(Co^{2+})^+$	315, 400	O_h $(Ni^{2+})^-$	385	g_1: 2.26 g_2: 2.10
	X-rays	$O_h(Co^{2+})^+$	315, 400	O_h $(Ni^{2+})^-$	385	g_1: 2.26 g_2: 2.10
FP4	XeHg lamp	Oh $(Co^{2+})^+$	–	O_h $(Ni^{2+})^+$	–	
	HOK lamp	O_h $(Co^{2+})^+$	–	O_h $(Ni^{2+})^+$	–	
	X-rays	O_h $(Co^{2+})^+$	295, 415	O_h $(Ni^{2+})^-$	370	g_1: 2.26 g_2: 2.10

[4] These bands arise probably due to O_h- and/or pseudo-tetrahedrally T_8-coordinated $(Ni^{2+})^+$ species.
[5] Extrinsic defects are hidden by intrinsic defects.

4.2 Dopants and solarization

Solarization was as a rule stronger in the doped than in the undoped base glasses. Defects in glasses doped with CoO and NiO can be explained as a combination of the defects found in the monodoped glasses. Co^{2+} was photooxidized to $(Co^{2+})^+$ in all glasses. Ni^{2+} with a lower redox potential than Co^{2+} showed a stronger dependency on the glass matrix. In the silicate and borosilicate glasses of the higher optical basicity range Ni^{2+} was photooxidized to $(Ni^{2+})^+$. However, in the phosphate and FP glasses with lower basicities, Ni^{2+} was even photoreduced to $(Ni^{2+})^-$. The extrinsic defects $(Co^{2+})^+$HC and $(Ni^{2+})^+$HC, formed by photooxidation, replaced partly intrinsic HC such as POHC, BOHC, H_I and H_{II}. The charge for the irradiation-induced $(Ni^{2+})^-$EC was balanced by an increased formation of intrinsic OHC. The coordination of the dopants also seems to be important for the defect formation, as octahedrally and tetrahedrally coordinated Ni^{2+} in the silicate and borosilicate glasses seem to exhibit different formation rates.

4.3 Glass matrix and solarization

The glass matrix determines not only the ease of intrinsic defect formation, which also influences the extrinsic defect formation, but also influenced the stability of the extrinsic defects.

Figures 11a and b illustrate the different strengths of defect formation in different model glasses by showing the maximal values of the induced extinction between 300 and 600 nm. Since not all glasses had any significant defects after irradiation with the XeHg lamp, and not all glasses were irradiated with the HOK lamp, the effects of both lamps are combined in figures 11a and b. The high differentiation of the defects is quite apparent in these figures and is based on the high selectivity of lamp excitation. The induced extinctions in the glasses containing Co^{2+} in tetrahedral coordination exceed any other observed defects by magnitudes. The intrinsic defects of the undoped (boro-)silicate glasses are distinctly smaller than in any of the doped glasses, while in the phosphate glasses the undoped and NiO-doped glasses have only a slightly lower induced extinction than the CoO-doped glasses. The general instability of the F-bonded defects can be seen in the lower rates of intrinsic defect formation in the FP glasses. The extent of solarization found after lamp irradiation reveals as a whole an increasing trend with increasing optical basicity of the glasses, which is also observed for the doped as well as the undoped glasses. For X-ray irradiation doped and undoped glasses indicate different trends. Figure 11b shows contrary to figure 11a that for the undoped glasses a stronger solarization is found in the FP and phosphate glasses when compared to the (boro-)silicate glasses.

X-ray irradiation of the doped glasses does not reflect the solarization of the base glass as seen after lamp irradiation. The amount of solarization seen in the doped glasses after X-ray irradiation complies strongly with the stability of the photoionized species and is thus clearly connected with the basicity of the glass matrix. The photooxidized $(Co^{2+})^+$ is more stabilized in the high-basicity glasses than in those of lower basicity. There is an exception in the basicity series when the matrix changes from a borosilicate to the phosphate glass where then the ease of the intrinsic defect formation pre-

vails over the pure basicity effect. The transition from the borosilicate to the phosphate glasses is even more severe for the NiO-doped glasses, as Ni^{2+} is photooxidized in the silicate glasses and photoreduced in the (fluoride-)phosphate glasses – the latter causing a stronger induced extinction with decreasing basicity of the FP glasses.

5. References

[1] Ehrt, D.; Seeber, W.: Glass for high performance optics and laser technology. J. Non-Cryst. Sol. **129** (1991) p. 19–30.

[2] Weyl, W.: Coloured glasses. Sheffield: Society of Glass Technology, 1951.

[3] Duffy, J. A.: A common optical basicity scale for oxide and fluoride glasses. J. Non-Cryst. Solids. **109** (1989) p. 35–39.

[4] Duffy, J. A.: Charge transfer spectra of metal ions in glass. Phys. Chem. Glasses **38** (1997) no. 6, p. 289–292.

[5] Seeber, W.: Kombination experimenteller und theoretischer Methoden der Absorptions- und Lumineszenzspektroskopie zur Entwicklung amorpher Materialien für Optik und Optoelektronik – Am Beispiel von Fluoridphosphatgläsern. Universität Jena, habilitation thesis 1995.

[6] Paul, A.; Douglas, R. W.: Optical absorption of divalent cobalt in binary alkali borate glasses and its relation to the basicity of glass. Phys. Chem. Glasses **9** (1968) no. 1, p. 21–26.

[7] Ehrt, D.; Ebeling, P.; Natura, U.: UV Transmission and radiation induced defects in phosphate and fluoride-phosphate glasses. J. Non-Cryst. Solids. **263 & 264** (2000) p. 240–250.

[8] Ebeling, P.; Ehrt, D.; Friedrich, M.: Study of radiation-induced defects in fluoride-phosphate glasses by means of optical absorption and EPR spectroscopy. Glastech. Ber. Glass Sci. Technol. **73** (2000) no. 5, p. 156–162.

[9] Ehrt, D.; Natura; U.; Ebeling, P.; et al.: Formation and healing of UV radiation defects in phosphate and fluoride phosphate glasses with high UV transmission. In: Proc. XVIII International Congress on Glass, San Francisco, CA (USA), 1998. Session C10, p. 1–6. (Available on CD-ROM from Am. Ceram. Soc.)

[10] Griscom, D. L.: Optical properties and structure of defects in silica glass. The Centennial Memorial Issue of J. Ceram. Soc. Jpn. **99** (1991) p. 923–942.

[11] Shkrob, I. A.; Tadjikov, B. M.; Trifunac, A. D.: Magnetic resonance studies on radiation-induced point defects in mixed oxide glasses. I. Spin centers in B_2O_3- and alkali borate glasses. II. Spin centers in alkali silicate glasses. J. Non-Cryst. Solids **262** (2000) p. 6–34 and p. 35–65.

[12] Möncke, D.; Ehrt, D.: Irradiation-induced defects in different glasses demonstrated on a metaphosphate glass. Glastech. Ber. Glass Sci. Technol. **74** (2001) no. 7, p. 199–209.

[13] Möncke, D.; Ehrt, D.: Radiation-induced defects in CoO- and NiO-doped fluoridephosphate glasses. Glastech. Ber. Glass Sci. Technol. **74** (2001) no. 3, p. 65–73.

[14] Möncke, D.; Natura, U.; Ehrt, D.: Radiation defects in CoO and NiO doped . glasses of different structure. In: Proc. 5th Conf. European Society of Glass Science and Technology (ESG), Prague 1999. Vol. B4, p. 49–56. (Available on CD-ROM from Czech Glass Society.)

[15] Natura, U.; Ehrt, D.: Formation of radiation defects in silicate and borosilicate glasses caused by UV lamp and excimer laser irradiation. Glastech. Ber. Glass Sci. Technol. **72** (1999) no. 9, p. 295–301.

[16] Bates, T.: Ligand field theory and absorption spectra of transition-metal ions in glasses. In: Mackenzie, J.D. (ed.): Modern aspects of the vitreous state. Vol.2. London: Butterworths, 1962. p. 195–255.

[17] Gan, F.; Deng, H.; Liu, H.: Paramagnetic resonance study on transition metal ions in phosphate, fluoridephosphate and fluoride glasses. Pt 2. Co^{2+} and Ni^{2+}. J. Non-Cryst. Sol. **52** (1982) p. 143–149.

[18] Pilbrow, J. R.: Transition ion electron paramagnetic resonance. Oxford: Clarendon, 1990. p. 327–331.

[19] Griscom, D. L.: Electron spin resonance in glasses. J. Non-Cryst. Solids **40** (1980) p. 211–272.

[20] Haines, R. I.; Mc Auley, A.: Synthesis and reaction of Ni(III) complexes. Coord. Chem. Rev. **39** (1981) p. 77–119.

[21] Lappin, G. A.; Murray, C. K.; Magerum, D. W.: Electron paramagnetic resonance studies of Ni(III).oligopeptide complexes. Inorg. Chem. **17** (1978) p. 1630–1634.

[22] Dietzel, A.; Coenen, M.: Über dreiwertiges Kobalt in Gläsern hohen Alkaligehaltes. Glastechn. Ber. **34** (1961) no. 2, p. 49–56.

[23] Stein, L.; Neil, J. M.; Alms, G. R.: Some properties of potassium hexafluoronickelates (III) and -(IV). Absorption spectra of Ni(III) and -(IV) in hydrogen fluoride solutions. Inorg. Chem. **8** (1969) p. 2472–2476.

[24] Westland, A. D.; Hoppe, R.; Kaseno, S. S. I.: Das magnetische Verhalten von Mischkristallen einiger binärer und ternärer Halogenide des Ni mit Mg. Z. anorg. allg. Chem. **338** (1965) p. 319–331.

[25] Nag, K.; Chakravorty, A.: Monovalent, trivalent and tetravalent nickel. Coord. Chem. Rev. **33** (1980) p. 87–147.

[26] Linhard, M.; Weigel, M.: Über Komplexverbindungen [Co(III)]. VII. Lichtabsorption von Mono- und Diacidoamminen des dreiwertigen Kobalts mit Fettsäureresten. Z. anorg. allg. Chem. **264** (1951) p. 321–335.

[27] Wentworth, R. A. D.; Piper, T. S.: A crystal field model for the relationships in monoacidopentamine and diacidotetramine complexes of cobalt (III). Inorg. Chem. **4** (1965) p. 709–714.

[28] Buxton, G. V.; Sellers, R. M.: Pulse radiolysis study of M^+ ions. J. Chem. Soc. Faraday Trans. **7** (1975) p. 558–567.

[29] Bowmaker, G. A.; Boyd, P. D.; Campbell, G. K. et al.: Spectroelectrochemical studies of Ni(I) complexes: One-electron reduction of nickel(II) complexes of dithiocarbamate and phosphine ligands $[Ni(R_2NCS_2)_x(Ph_2PCH_2CH_2PPh_2)_{2-x}]^{2-x}$ (x = 0,1,2). Inorg. Chem. **21** (1982) p. 1152–1159.

[30] Sreeramachandra Prasad, L.; Subramanian, S.: E.P.R. of Ni(I) radiolytically produced in Ni(II)doped Cd(imidazole)$_3SO_4H_2O$. Mol. Phys. **57** (1986) no. 3, p. 543–552.

[31] Robroeck, L. van; Goovaerts, E.; Schoemaeker, D.: Electron-spin-resonance study of Co^{2+} and Ni^+ centers in AgCl (Cu, Co, Ni). Phys. Stat. Sol. (b) **132** (1985), p. 179–187.

Contact:

Dr. Doris Möncke
Otto-Schott-Institut für Glaschemie
Friedrich-Schiller-Universität Jena
Fraunhoferstraße 6
D-07743 Jena

E-mail: dorismoencke@web.de